



Effective Management of Brainstem Tumors: A Study of 22 Patient Experiences

Ersin HACIYAKUPOGLU¹, Evren YUVRUK², Ayca Ersen DANYELI³, Sebahattin HACIYAKUPOGLU⁴

¹Heinrich-Braun-Klinikum, Zwickau, Department of Neurosurgery, Zwickau, Germany

²Umraniye Education and Research Hospital, Department of Neurosurgery, Istanbul, Türkiye

³Acibadem University, School of Medicine, Department of Medical Pathology, Istanbul, Türkiye

⁴Acibadem University, School of Medicine, Department of Neurosurgery, Adana, Türkiye

This study has been presented at the 37th Scientific Congress of the Turkish Neurosurgical Society between 18 and 21 April, 2024 at Antalya, Türkiye

Corresponding author: Ersin HACIYAKUPOGLU ✉ haciyakupoglu@yahoo.com

ABSTRACT

AIM: To evaluate the surgical outcomes, extent of resection, and postoperative clinical improvement in 22 patients with brainstem tumors.

MATERIAL and METHODS: We performed surgery on 22 patients with brainstem tumors using various approaches to access the pathology. Our goal was to achieve gross total resection wherever feasible, although this was not possible in all cases. Spontaneous breathing was preferred during surgery, and resection was halted if any disturbance occurred. Bipolar or monopolar coagulation was avoided, and smooth compression and irrigation were used for bleeding control. Neuromonitoring was employed during surgery for all patients.

RESULTS: Among the 22 patients included in this study, 4 presented with long tract symptoms, 3 had hydrocephalus, 5 had papillary stasis, 4 had cerebellar findings, 3 had gait disturbances, 1 had respiratory disturbance, and 1 had dysphagia. Gross total resection was achieved in 10 patients, near-total resection in 4, and partial resection in 8.

CONCLUSION: Surgery enables histologic diagnosis, relieves mass effect, and improves symptoms in brainstem tumors. While gross total resection is ideal, it should not be insisted on in infiltrative tumors; partial or subtotal resection may provide long-term benefit in focal and exophytic lesions. Careful neuromonitoring and anatomical planning are essential to minimize morbidity.

KEYWORDS: Brainstem tumors, Exophytic, Focal, Diffuse, Infiltrative

ABBREVIATIONS: **CNS:** Central nervous system, **NF1:** Neurofibromatosis type 1, **NF2:** Neurofibromatosis type 2, **VA:** Vertebral artery, **BA:** Basilar artery, **PICA:** Posterior inferior cerebellar artery, **BST:** Brainstem tumor, **GBM:** Glioblastoma multiforme, **GTR:** Gross total resection, **DIPG:** Diffuse intrinsic pontine glioma, **MRI:** Magnetic resonance imaging, **PNET:** Primitive neuroectodermal tumor, **RT:** Radiotherapy, **HE:** Hematoxylin and eosin, **GCS:** Glasgow coma scale

INTRODUCTION

Approximately 5% of all intracranial tumors and 25% of posterior fossa tumors arise in the brainstem, with 80% located in the pons and 86% of those histologically classified as diffuse infiltrative fibrillary astrocytoma grade II

(6,11,23). Although these tumors are typically classified as low-grade histologically, they frequently behave like supratentorial high-grade gliomas in children, demonstrating infiltrative, aggressive, and progressive characteristics, with no clear demarcation lines and symmetrical metastasis in vertical and transverse directions (11,18,23).

Ersin HACIYAKUPOGLU : 0000-0002-9712-9913
Evren YUVRUK : 0000-0002-2945-743X

Ayca ERSEN DANYELI : 0000-0001-8015-9916
Sebahattin HACIYAKUPOGLU : 0000-0002-0700-7593



This work is licensed by "Creative Commons Attribution-NonCommercial-4.0 International (CC)".

Brainstem tumors (BSTs) are most commonly detected in children, particularly males; moreover, these tumors often remain asymptomatic until they reach a significant size due to their midline location (7,28). The most common symptoms of BSTs include headache, vomiting, and gait disturbances, whereas the most prominent clinical findings include papilledema, ataxia, strabismus, nystagmus, vertigo, cranial nerve deficits, long tract signs, and head bobbing (27,28). In cases with hydrocephalus, shunt procedures may be required (2).

Approximately 90% of BSTs originate from astrocytic lineage and include diffuse fibrillary, pilocytic, pilomyxoid, pleomorphic xanthoastrocytoma, and other histological variants (11,19). The less frequent pathologies include oligodendroglioma, ependymoma, primitive neuroectodermal tumor (PNET), atypical teratoid/rhabdoid tumor (AT/RT), hamartoma, tuberculoma, and fungal granulomas (9,10,14).

Based on anatomical and radiological characteristics, BSTs may be classified as focal, anterior, posterior, lateral, exophytic, diffuse, infiltrative, or intrinsic (18). Magnetic resonance imaging (MRI) is the most preferred imaging modality for BSTs as it provides valuable data on their localization, extent, neighborhood, and differential diagnosis (8,18,32).

Focal exophytic midbrain, medullary, and cervicomedullary tumors can be treated via gross total resection (GTR), whereas diffuse infiltrative pontine gliomas (DIPGs) without an exophytic component cannot be treated surgically (23). Instead, these lesions can be treated using radiotherapy, chemotherapy, immunologic therapies, stereotactic radiosurgery, genetic therapies, and targeted molecular agents including IL-13 receptor-targeted approaches (13,15,16,22).

In this study, we evaluated 22 patients with brainstem tumors who had undergone surgical treatment between 2010 and 2023. We analyzed their outcomes based on the extent of resection—gross total, near-total, or partial—and assessed the role of follow-up in stable lesions. A comprehensive literature review was also performed.

■ MATERIAL and METHODS

Of the 22 BSTs analyzed in this study, 3 were located in the midbrain and 2 in the peduncle. These five tumors were resected through pterional craniotomy. We reached the tumor after opening the Sylvian fissure, opticocarotid complex, and carotico-oculomotor triangle (Figure 1).

A tectal tumor was removed using the occipital transcallosal approach by splitting the splenium.

We resected three DIPGs; of these, two were ventral exophytic tumors that were resected through pterional craniotomy and by opening the prechiasmatic and interpeduncular cisterns (21). We used a thin-tipped ultrasonic suction tube to partially resect the tumor. In a patient with a posterior exophytic tumor, subependymal protrusion and portions obstructing the aqueduct were surgically removed using a classic posterior fossa approach through the cisterna magna, involving partial vermis splitting (22). The same procedure was used for four posterior exophytic medullary tumors. We resected 1/3 of the bottom part of the vermis (18). The same approach was used for two focal medullary tumors subjected to GTR. Three lateral exophytic medullary tumors were accessed through posterolateral incision and retromastoid craniotomy, similar to the approach used for pontocerebellar angle (PCA) tumors (25).

We did not perform a midline incision into the floor of the fourth ventricle. Furthermore, we did not descend beyond the base of the fourth ventricle, unless necessary (21). The tumor was resected from the center to the periphery (Figure 2).

If there was uncertainty regarding tissue identification, a frozen section was performed; meanwhile, the patient was monitored, and a stimulator was used (28). We preferred spontaneous respiration in all cases. If any alteration in respiratory or cardiac rhythm was observed, the surgery was stopped and resumed after recovery.

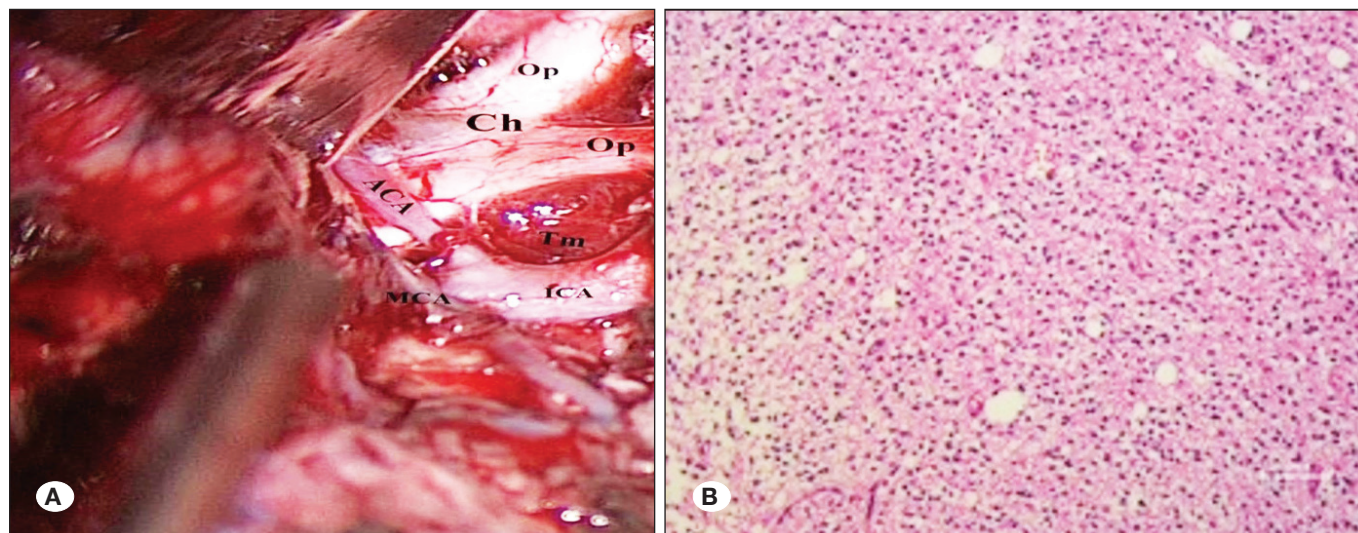


Figure 1: **A)** Surgical exposure via prechiasmatic, opticocarotid, and cortico-oculomotor triangle. **B)** Astrocytoma composed of fibrillary astrocytic cells with cytoplasm and fusiform nuclei. Hematoxylin and eosin (H&E) staining, $\times 100$.

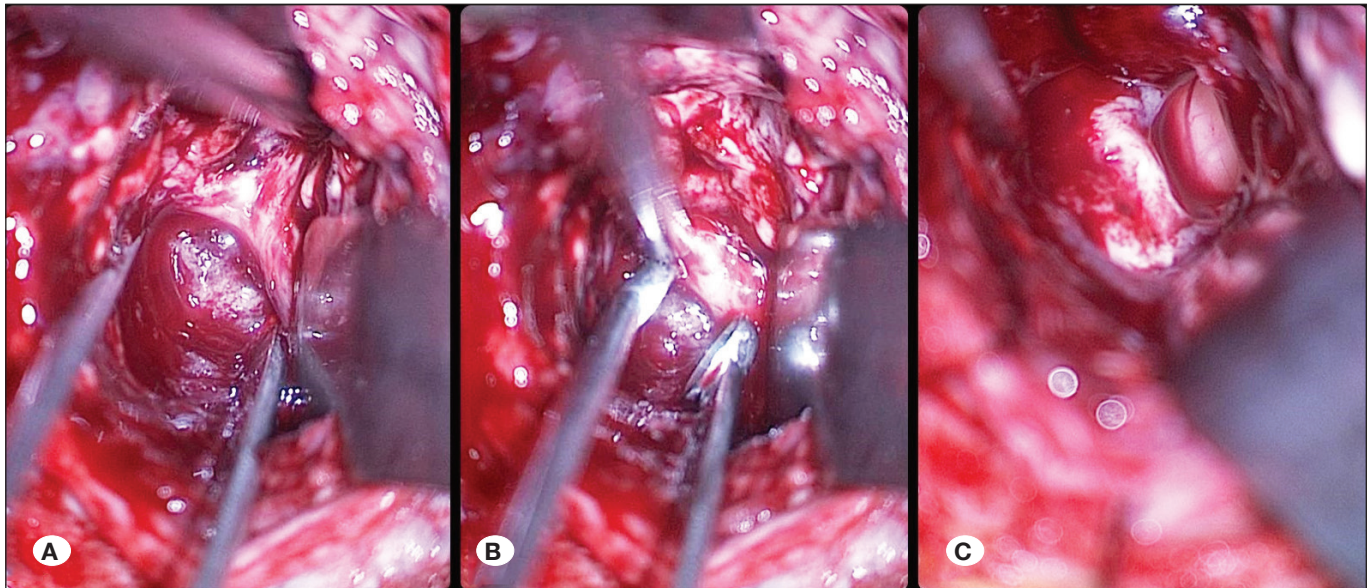


Figure 2: Patient #11. Piecemeal removal of the tumor from center to periphery; no glial barrier observed, consistent with infiltrative growth.

We gained access to the tumor through a cystic, discolored, protruding area with abnormal vascularization, choosing the shortest route to reach the exophytic region (22). We avoided the use of laser and bipolar cautery whenever possible. Bleeding ceased after applying gentle pressure with a wet cotton compress. Seven cervicomedullary tumors were surgically excised via a midline incision, adhering to standard microsurgical guidelines for accessing the fourth ventricle. However, a midline approach was not used for all cases; instead, a mediolateral approach was used when a protruding cystic area was present (28).

This retrospective study was conducted in accordance with the principles of the Declaration of Helsinki (32). All surgical and diagnostic procedures had been performed under the standard institutional regulations in place at the time of treatment, and written informed consent had been obtained from all patients and/or their legal guardians.

■ RESULTS

In 3 of the 22 patients with BSTs, the tumors were located in the midbrain. One patient with a tectal tumor was 35 years old and had papillary stasis and Parinaud's syndrome. In this patient, GTR was performed, and he was pathologically diagnosed with mature teratoma. The conditions resolved postoperatively. The other two patients were 3- and 7-year-old girls with a peduncular tumor who were pathologically diagnosed with pilocytic astrocytoma. Their symptoms, i.e., headache, nausea, and vomiting, improved after partial resection.

Two male patients aged 3 and 4 years had ventral exophytic DIPGs. One patient had primary optic atrophy, hydrocephalus, and a Glasgow Coma Scale (GCS) score of 5. In this patient, partial resection was performed and a V-P shunt was inserted for hydrocephalus. This patient was pathologically

diagnosed with pilocytic astrocytoma and was found to gain consciousness postoperatively. However, the other patient showed no neurological symptoms, underwent partial resection, and was pathologically diagnosed with astrocytoma grade II.

A 6-year-old male patient with a dorsal exophytic DIPG had hydrocephalus and gait disturbance. After partial resection, the hydrocephalus improved. He was pathologically diagnosed with astrocytoma grade II.

Four patients had dorsal exophytic medullary focal tumors. The first patient was a 38-year-old man with cerebellar findings. He underwent GTR and was pathologically diagnosed with glioblastoma multiforme (GBM). The second patient was an 18-year-old woman with hydrocephalus and papillary stasis. She underwent GTR and was pathologically diagnosed with GBM. The third patient was a 21-year-old woman with cerebellar findings. She underwent near-total resection and was pathologically diagnosed with GBM. The fourth patient was an 11-year-old boy with multiple cranial nerve paralysis, gait imbalance, and diplopia. He underwent GTR and was pathologically diagnosed with ganglioglioma.

Three patients had lateral exophytic focal medullary tumors. The first patient was a 3-year-old girl with hydrocephalus and papillary stasis. She underwent GTR and was pathologically diagnosed with ependymoma. The second patient was a 4-year-old boy with hemiparesis and strabismus. He underwent partial resection and was pathologically diagnosed with ependymoma. The third patient was a 9-year-old boy with gait disturbance. He underwent partial resection and was pathologically diagnosed with pilocytic astrocytoma.

Two patients with focal medullary tumors underwent GTR. One patient was an 8-year-old boy with imbalance and diplopia who was pathologically diagnosed with astrocytoma grade II (Figure 3).

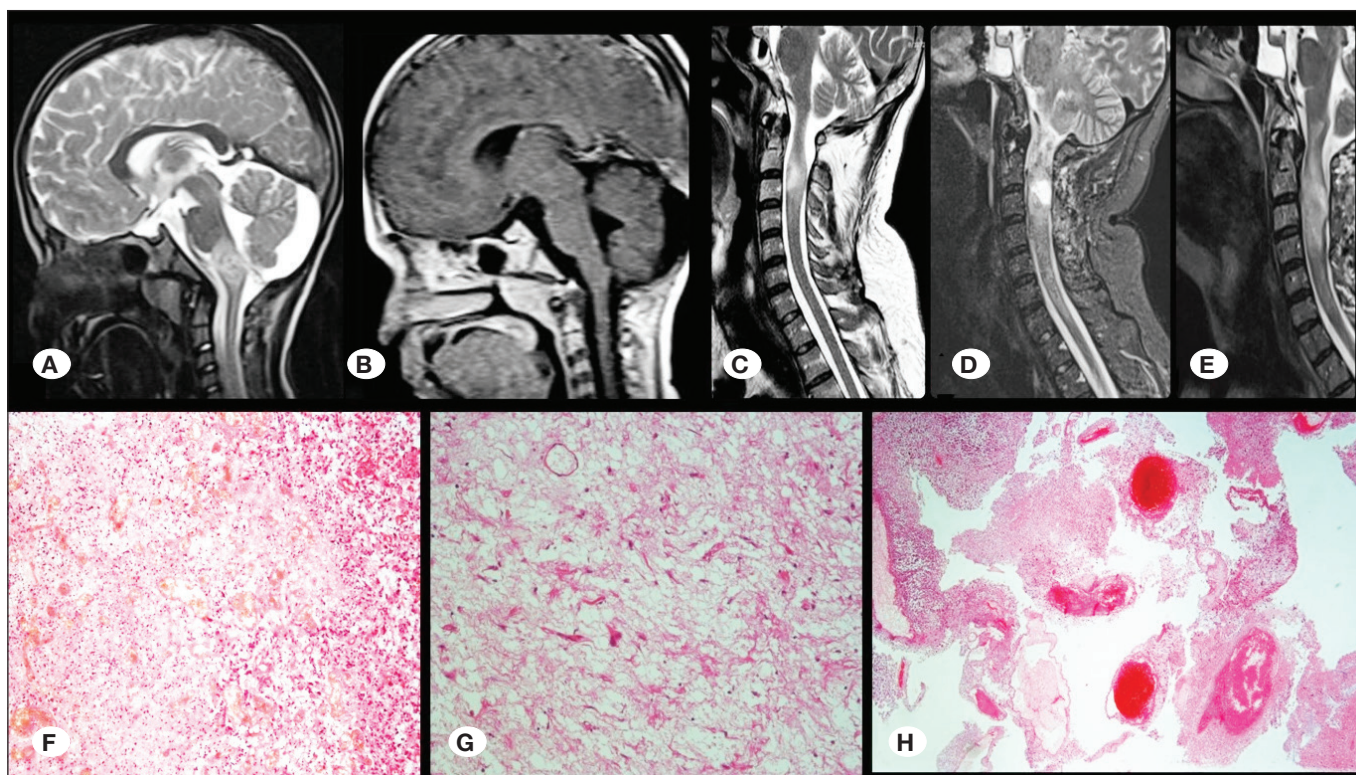


Figure 3: Patient #16. Focal medullary tumor, preoperative (A) and postoperative (B) MRI scans. Cervicomedullary Glioblastoma multiforme (GBM), preoperative (C, D) and postoperative (E) views. F) GBM, Hematoxylin and Eosin (H&E) staining, $\times 200$. G) GBM, immunohistochemical staining, $\times 200$. H) Thrombus mass in a dilated vessel of GBM, H&E, $\times 200$, consistent with vascular invasion.

The other patient was a 13-year-old girl with gait disturbance who was pathologically diagnosed with oligodendroglioma.

Seven patients had cervicomedullary tumors. The first patient was a 27-year-old man with quadriplegia and respiratory disturbance. He underwent near-total resection and was pathologically diagnosed with GBM. His findings improved, except for the mild left hemiparesis. On postoperative day 2, he experienced irregular nocturnal breathing, which occurred at 7–8-h intervals. Breathing was supported, but the residual tumor quickly expanded to the distal and proximal areas. The patient died on postoperative day 75 due to respiratory arrest.

The second patient was a 20-year-old man with arm weakness. He underwent GTR and was pathologically diagnosed with GBM. The third patient was a 7-year-old girl with dysphagia. She underwent GTR and was pathologically diagnosed with pilocytic astrocytoma. Her condition improved in 1 week (Figure 4).

The fourth patient was a 4-year-old girl with papillary stasis and hydrocephalus. She underwent GTR and was pathologically diagnosed with ependymoma. Her pathological findings improved after GTR. The fifth patient was a 5-year-old girl with hemiparesis. She underwent partial resection and was pathologically diagnosed with astrocytoma grade II. Her hemiparesis improved after partial resection. The sixth patient was a 41-year-old man with papillary stasis and quadriplegia who was pathologically diagnosed with ependymoma (Figure 5).

The seventh patient was a 38-year-old man with quadriplegia, left spasmodic torticollis, and glossopharyngeal neuralgia. He underwent GTR and was pathologically diagnosed with hemangioblastoma. We accessed the saccular aneurysm at the origin of the posterior inferior cerebellar artery by following the left vertebral artery. His conditions improved postoperatively (Figure 6).

Except for the children, all patients suffered from headache and vomiting. The study population consisted of 22 patients, including 12 female and 10 male patients. Of them, eight were adults (mean age: 29.8 years) and four were children (mean age: 6.2 years). The mean age of all patients was 14.7 years.

Of the 22 patients in this study, 4 had long tractus symptoms, 3 had hydrocephalus, 5 had papillary stasis, 4 had cerebellar findings, 3 had gait disturbance, 1 had respiratory disturbance, and 1 had agglutination. Ten, four, and eight patients underwent GTR, near-total resection, and partial resection, respectively.

The detailed demographic and clinical characteristics of all 22 patients are summarized in Table I.

DISCUSSION

Advances in anesthesia and asepsis led to significant improvements in abdominal and thoracic surgeries during the 19th century. However, brain tumor surgery could not be significantly improved because it is difficult to accurately localize these tumors (9). In 1884, Richman Godlee localized an IC

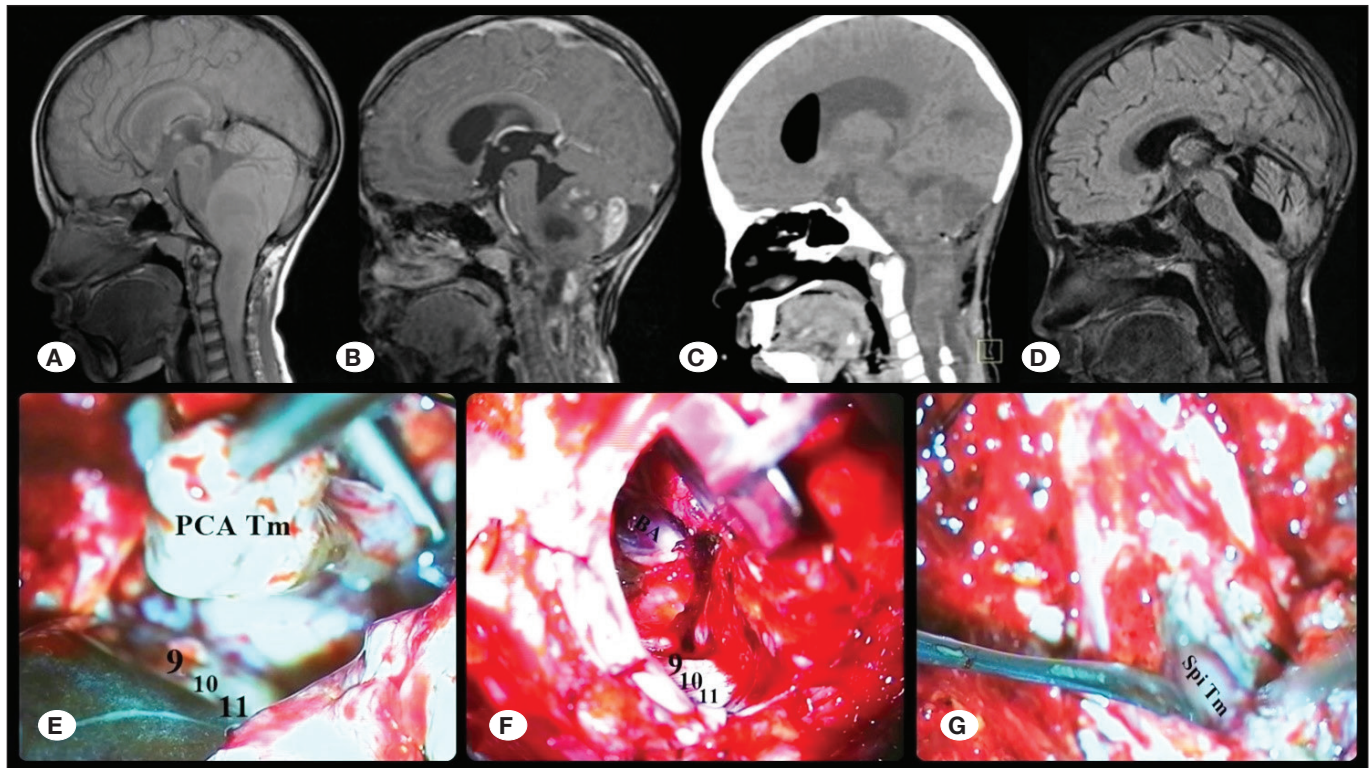


Figure 4: Patient #18. Pilocytic astrocytoma extending to the fourth ventricle, posterior cranial area (PCA), and cervicomedullary region. **A)** Preoperative T1W sagittal MR imaging. **B)** Multiple cystic structures and heterogeneous contrast enhancement in T1W sagittal MR image. **C)** Early postoperative CT scan. **D)** Late postoperative period (1 year after surgery). **E–G)** Cervicomedullary tumor with exophytic lateral extension into the PCA; postoperative follow-up shows resolution of hydrocephalus and gait disturbance.

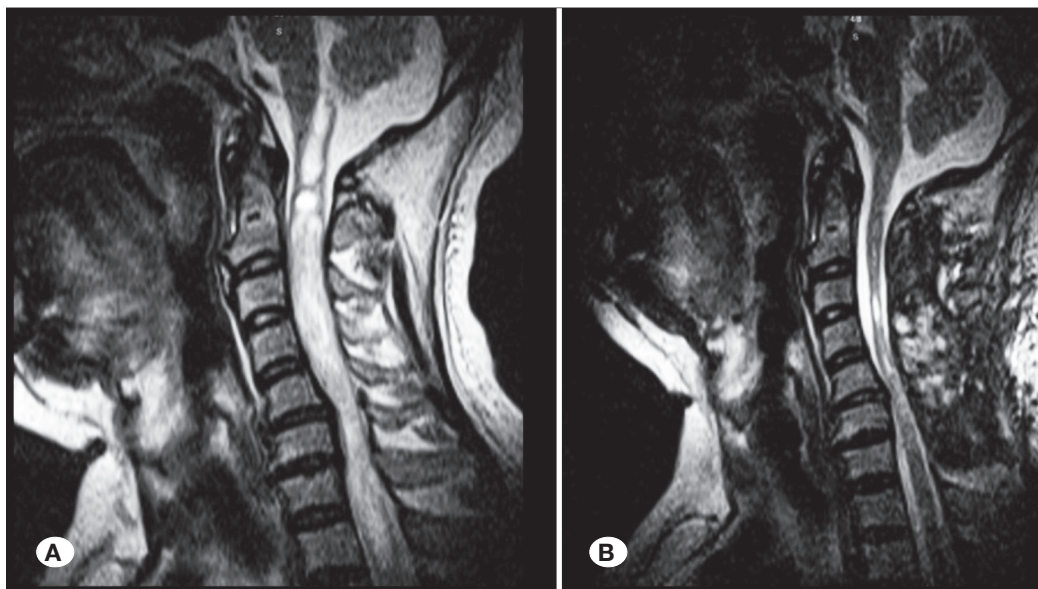


Figure 5: (Patient #19) T2W sagittal MRI scans. Preoperative (**A**) and postoperative (**B**).

tumor in a patient with focal epilepsy through neurological examination and performed a successful operation (17). During this period, some brave surgeons attempted to treat desperate patients through craniotomy; however, most of them were unsuccessful as they could not localize the lesion (15). In the 1950s, advancements in neurology deepened our un-

derstanding of brain anatomy and physiology. Consequently, a significant increase in the rates of intracranial tumor surgery and GTR was observed, except for BSTs (3). At the end of the 20th century, advancements in imaging techniques allowed for precise tumor localization and a preliminary understanding of its histological characteristics (9). Furthermore, advances in

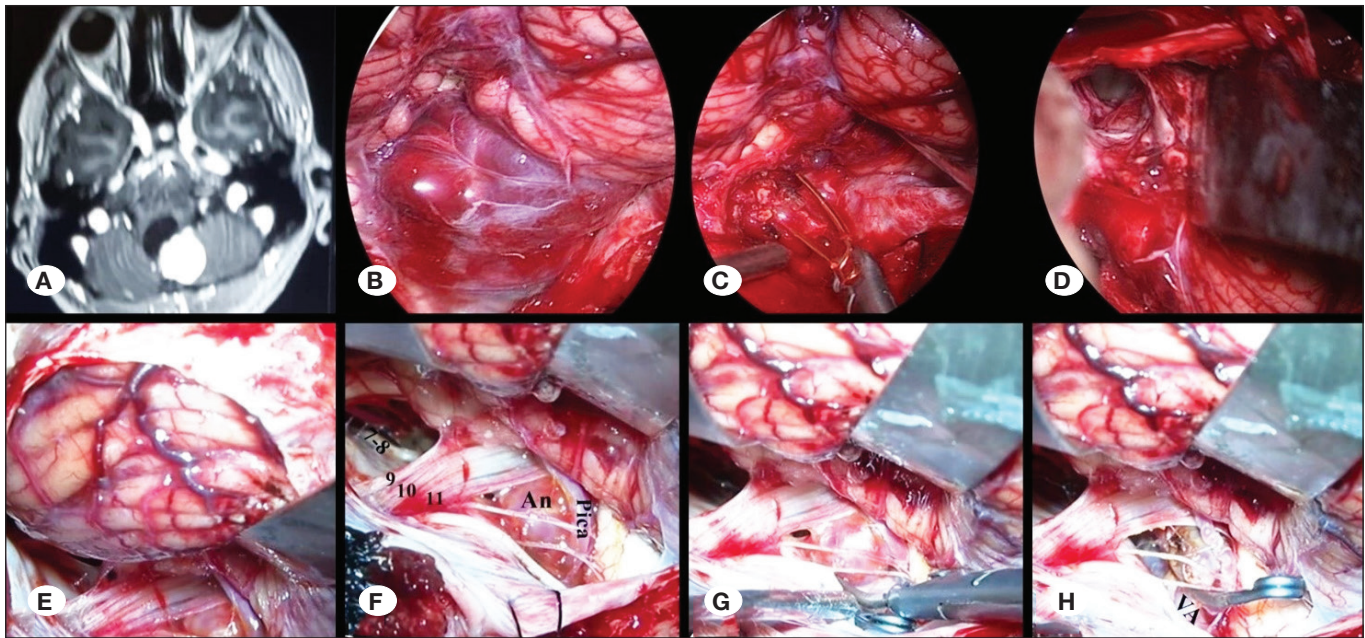


Figure 6: Patient #22. **A)** Preoperative axial contrast enhanced T1W MRI, **B–D)** Cervicomedullary hemangioblastoma in operative micrographs. **E–H)** PICA aneurysm coexisting with cervicomedullary hemangioblastoma. Complete removal of the hemangioblastoma and associated PICA aneurysm confirmed.

Table I: Detailed Demographic and Clinical Characteristics of All 22 Patients

Case	Age (years)	Sex	Tumor Location	Surgical Approach	Extent of Resection	Histopathology
1	35	F	Midbrain	Posterior transcallosal	GTR	Teratoma
2	3	F	Peduncle	Pterional	Partial	Pilocytic astrocytoma
3	7	F	Peduncle	Pterional	Partial	Pilocytic astrocytoma
4	3	M	Pons	Pterional	Partial	Pilocytic astrocytoma
5	4	M	Pons	Pterional	Partial	Astrocytoma, WHO Grade II
6	6	M	Pons	Posterior fossa	Partial	Astrocytoma, WHO Grade II
7	38	M	Medulla	Posterior fossa	GTR	GBM
8	18	F	Medulla	Posterior fossa	GTR	GBM
9	21	F	Medulla	Posterior fossa	Near-total	GBM
10	11	M	Medulla	Posterior fossa	GTR	Ganglioglioma
11	3	F	Medulla	Retromastoid	GTR	Ependymoma
12	4	M	Medulla	Retromastoid	Partial	Ependymoma
13	9	M	Medulla	Retromastoid	Partial	Pilocytic astrocytoma
14	8	M	Medulla	Posterior fossa	GTR	Astrocytoma, WHO Grade II
15	13	F	Medulla	Posterior fossa	GTR	Oligodendroglioma
16	27	M	Cervico-medullary	Posterior fossa	Near-total	GBM
17	20	M	Cervico-medullary	Posterior fossa	GTR	GBM
18	7	F	Cervico-medullary	Posterior fossa	GTR	Pilocytic astrocytoma
19	4	F	Cervico-medullary	Posterior fossa	GTR	Ependymoma
20	5	F	Cervico-medullary	Posterior fossa	Partial	Astrocytoma, WHO Grade II
21	41	M	Cervico-medullary	Posterior fossa	GTR	Ependymoma
22	38	M	Cervico-medullary	Posterior fossa	GTR	Hemangioblastoma

GBM: Glioblastoma multiforme, **GTR:** Gross total resection

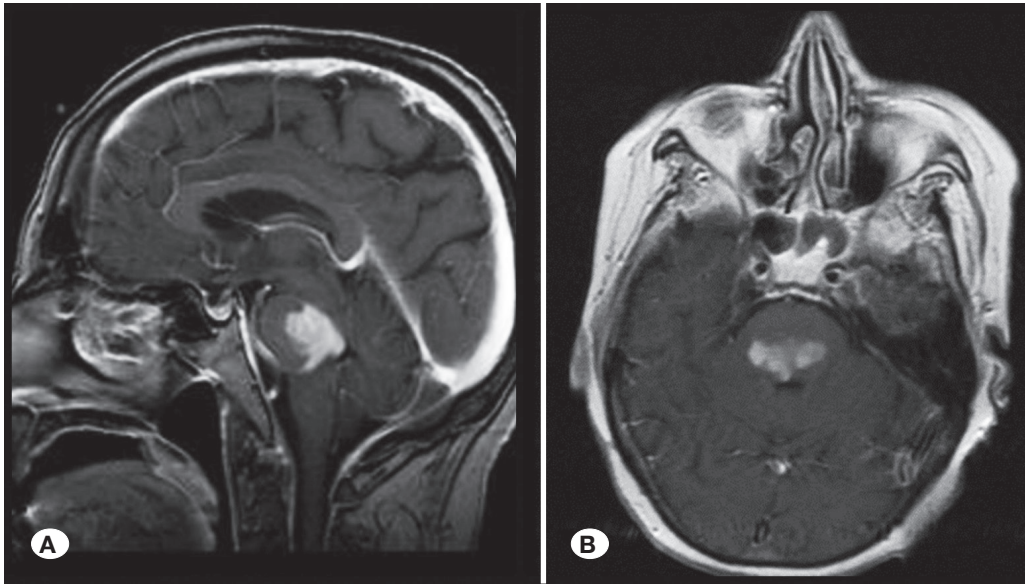


Figure 7: Sagittal (A) and axial (B) T1W contrast enhanced MR images show symmetric expansion of DIPGs in both transverse and vertical planes [image(s) courtesy of the authors' archive].

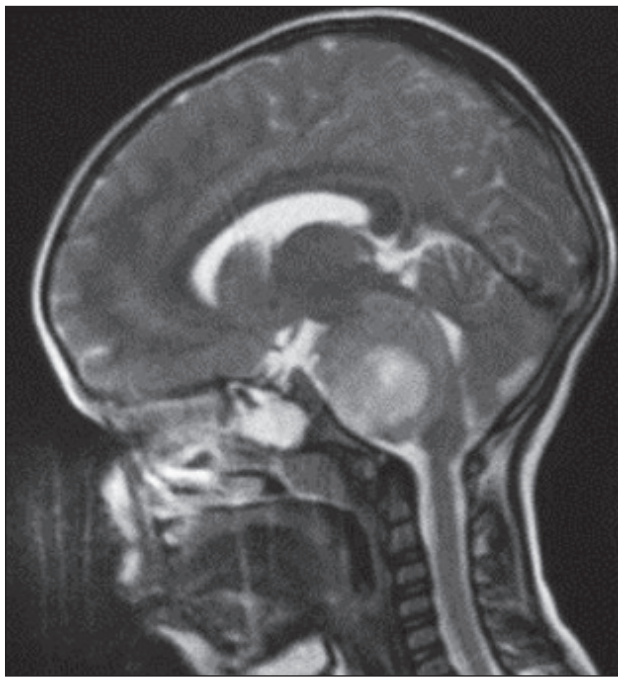


Figure 8: Enlarged (fat) pons [image(s) courtesy of the authors' archive].

microsurgical instruments increased the likelihood of a successful surgery. However, no success has been observed in the treatment of BSTs because most of them are diffuse, aggressive, highly invasive, infiltrative, and malignant. Moreover, they lack clear demarcation and are surrounded by normal tissues, leading to a high recurrence rate (17). BSTs exhibit life-threatening, extensive, and critical anatomical structures and progress rapidly. Furthermore, determining a functional entrance route to reach the tumor is challenging (15,17).

The brainstem contains corticopedal and corticofugal pathways, projection tracts, nuclei of the reticular formation, and

centers responsible for respiratory and cardiovascular functions (24). It plays a pivotal role in muscle tonus, consciousness, awareness, and regulation of motor responses to stimuli (15). The nuclei of all cranial nerves and neurons, except for the first two cranial nerves, are settled in the brainstem (24).

Catecholamine, indolamine, enkephalin, and many other neurotransmitters are secreted from the brainstem. Therefore, currently, these tumor types are not treated via surgery (24).

In the 2000s, developments in MRI technologies, including diffusion tensor imaging, functional MRI, spectroscopic MRI, and diffusion MRI, allowed for precise identification of brainstem tumors, their cellular characteristics, surrounding tissues, and functional access points (10). During operation, the use of MRI, ultrasound (USG), somatosensory evoked potential, motor evoked potential (12), multimodality evoked potential, and nerve and nucleus stimulation along with neuronavigation assistance enables successful BST resection and minimizes morbidity and mortality (28).

Sulci, gyri, and a functional area at the base of the fourth ventricle do not develop before the age of 4 years (6,15). Furthermore, cortical stimulation is inexcitable before the age of 8 years. Therefore, navigation (mapping) cannot be performed. Since 75% of BSTs develop in children, problems remain unsolved (1,8).

In DIPGs, which constitute 80% of BSTs, surgery is not indicated if the exophytic component is absent. Although approximately 86% of DIPGs in children are histologically classified as diffuse infiltrative fibrillary astrocytoma grade II (15), these tumors often behave like supratentorial high-grade gliomas in the pediatric population. They are infiltrative, aggressive, and progressive in nature, lacking encapsulation or clear demarcation lines, and tend to spread symmetrically in both vertical and transverse directions (15,28) (Figure 7).

If RT is not applied, malignant transformation does not occur. Pons enlarges (fat pons) (Figure 8). The midbrain, medulla, and

peduncles sometimes have an anterior exophytic component and rarely a posterior exophytic component (31).

It pushes the fourth ventricle back and causes a subependymal bulging at the rhomboid fossa (Figure 9).

Subarachnoid spread occurs and envelops at the vertebral artery (VA) and basilar artery (BA) in 50% of the patients (19,31). Tumor may spread to the prepontine, interpeduncular, prechiasmatic, and suprachiasmatic cisterns and diencephalon. It spreads through fibers and attaches to critical areas. It can be cystic, and focal growth may develop in 10% of cases. Furthermore, leptomeningeal infiltration may be detected in 5%–25% of cases, which can often lead to death in a short time. Spontaneous regression can also occur occasionally (31) (Figure 10).

Pilocytic astrocytoma in the pons is the second most frequently observed tumor. Dysembryoplastic neuroepithelial tumor, PNET, AT/RT, ependymoma, and primary and secondary GBM

can also be detected (25). Hemisphere tumors can infiltrate the pons (20) (Figure 11).

In 2018, we encountered a case of a patient with DIPG who had hydrocephalus. The tumor had spread to the prepontine prechiasmatic cistern. His GCS score was 5, and due to his unconscious state, a ventricular drain was inserted. He was later discharged from the hospital as he could not be operated. Subsequently, he was admitted to our hospital and subjected to ventriculoperitoneal shunt, pterional craniotomy, and Sylvian dissection. We explored the tumor through the triangular opening of opticocarotid and carotico-oculomotor. Tumor tissues in the cisterns were removed using a thin pointed ultrasonic suction until the BA was seen (9) (Figure 12).

The patient regained his consciousness and was discharged from the hospital on the 10th day. He underwent chemotherapy and was pathologically diagnosed with pilocytic astrocytoma. He has been living without assistance for the last 5 years.

However, it was noted that attempting resection would provide minimal benefit. We partially resected one ventral exophytic pontine tumor and two midbrain peduncular tumors using the same approach, without any complication. The pathological diagnosis of the DIPG was astrocytoma grade II, whereas the peduncular tumors were diagnosed as pilocytic astrocytoma. Although 5% of pilocytic astrocytomas are reportedly associated with neurofibromatosis types I and II (NF1 and NF2), none of our cases presented with NF. Peduncular tumors can be removed using the infratemporal approach, which involves opening the tentorium through the corridor inside the transchoroidal fissure; however, we do not have any experience in this approach (20).

A DIPG with a posterior exophytic component at the left superior fossa occluded the aqueduct entrance of the fourth ventricle and resulted in hydrocephalus. To reach the lesion, we nearly had to totally separate the cerebellar vermis. In patients who undergo total vermis separation, mutism can develop due to the dentato rubro thalamic tract lesion; however, we

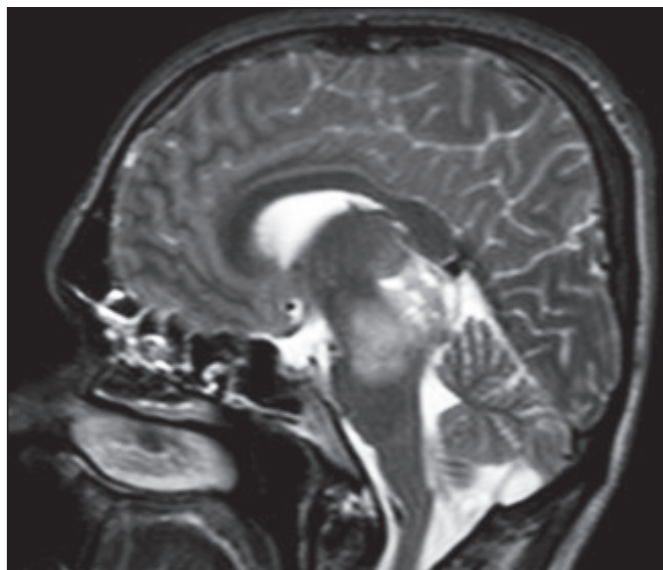


Figure 9: Infiltration of a tectal tumor into the pons [image(s) courtesy of the authors' archive].

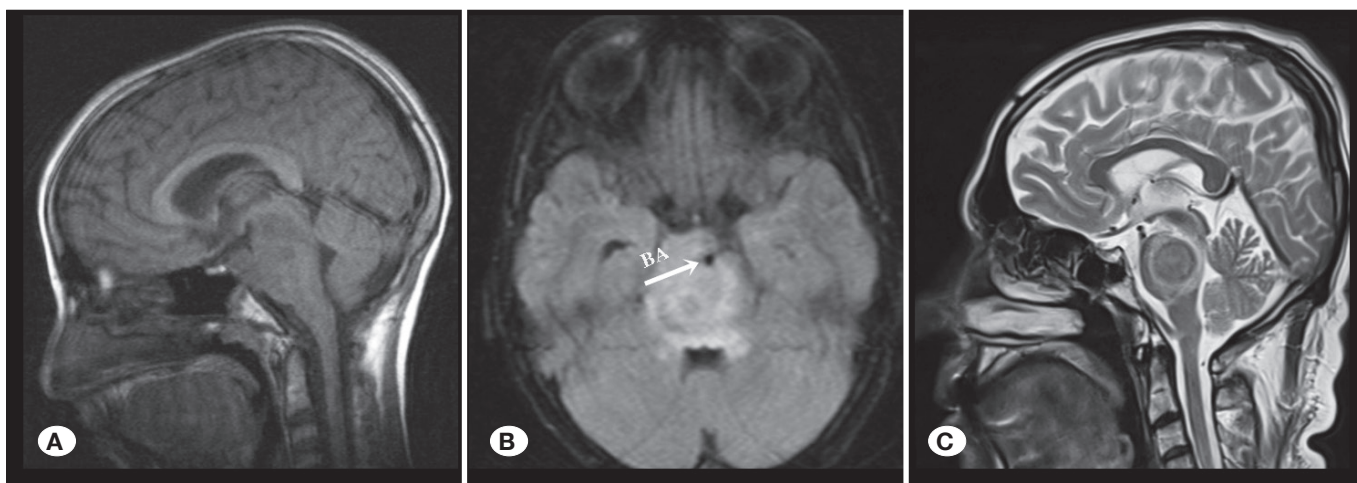


Figure 10: Infiltration of a ventral exophytic pontine tumor into the midbrain and medulla; basilar artery (BA) surrounded [image(s) courtesy of the authors' archive].

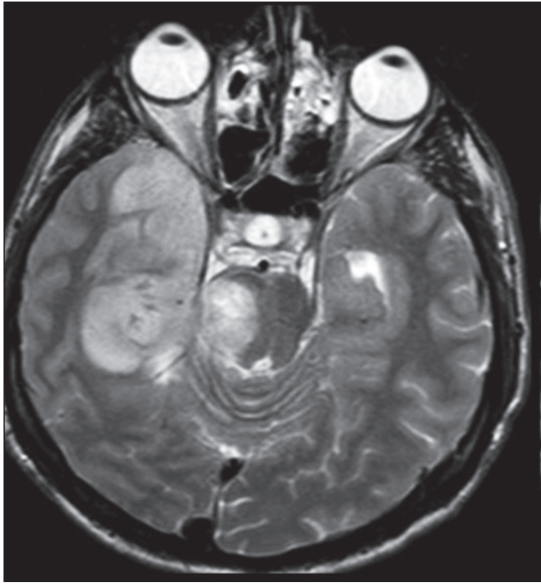


Figure 11: Infiltration of a hemispheric tumor into the pons [image(s) courtesy of the authors' archive].

did not detect mutism in any of our cases (1,23). We opened the subependymal and obliterated parts of the aqueduct. No additional neurological deficit developed. The pathological diagnosis was diffuse fibrillary astrocytoma grade II.

Midbrain tectal tumor is rare and exhibits an indolent course if hydrocephalus is absent (18). Surgical management of these tumors requires careful planning and proper technical approaches (30). A 35-year-old woman had headache, hydrocephalus, and Parinaud's syndrome. She underwent GTR, in which the splenium was opened using the posterior transcallosal approach, and was pathologically diagnosed with teratoma. Her conditions improved postoperatively (12) (Figure 13).

Small tectal tumors have a high likelihood of being hamartomas; moreover, they can be indolent for a long time. We followed up three patients for 10 years and no changes were observed during the follow-up (6,10) (Figure 14).

Most tectal tumors are astrocytomas and have an indolent course (5). They can be cystic, low-grade, and anaplastic

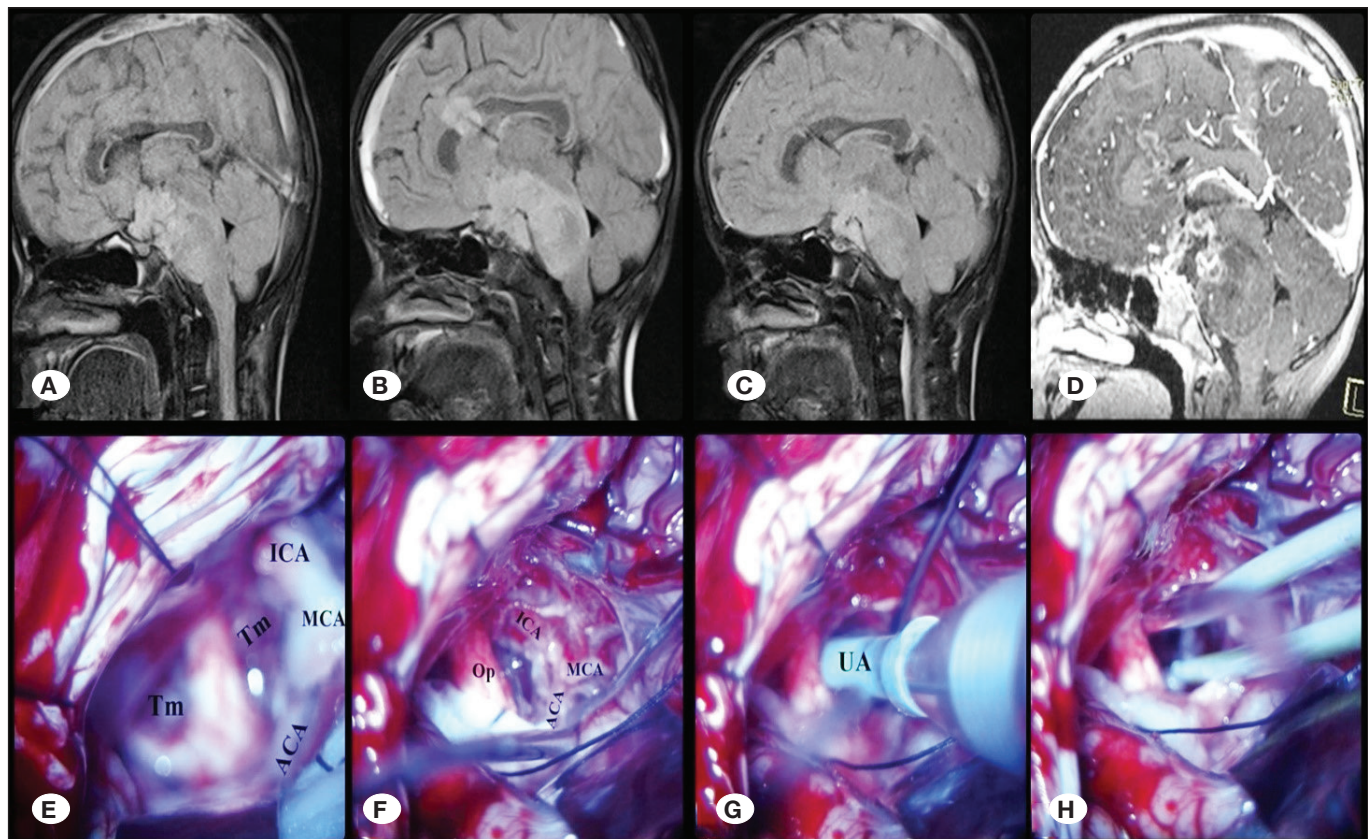


Figure 12: Patient #3. **A)** Preoperative sagittal T1-weighted MRI demonstrating the brainstem tumor. **B)** Preoperative sagittal MRI showing the lesion and its relationship to the surrounding structures. **C)** Early postoperative sagittal MRI confirming decompression of the brainstem and adequate tumor debulking. **D)** Late postoperative sagittal MRI at follow-up demonstrating stable postoperative changes without radiological progression. **E)** Intraoperative microscopic view after pterional craniotomy and Sylvian fissure dissection, showing the tumor (T) and surrounding vascular structures (ICA, MCA). **F)** Intraoperative view demonstrating further tumor exposure and debulking within the operative field. **G)** Intraoperative view showing the ultrasonic aspirator (UA) in the prechiasmatic cistern, used for piecemeal tumor removal. **H)** Final intraoperative view after debulking, illustrating decompression of the critical neurovascular structures.

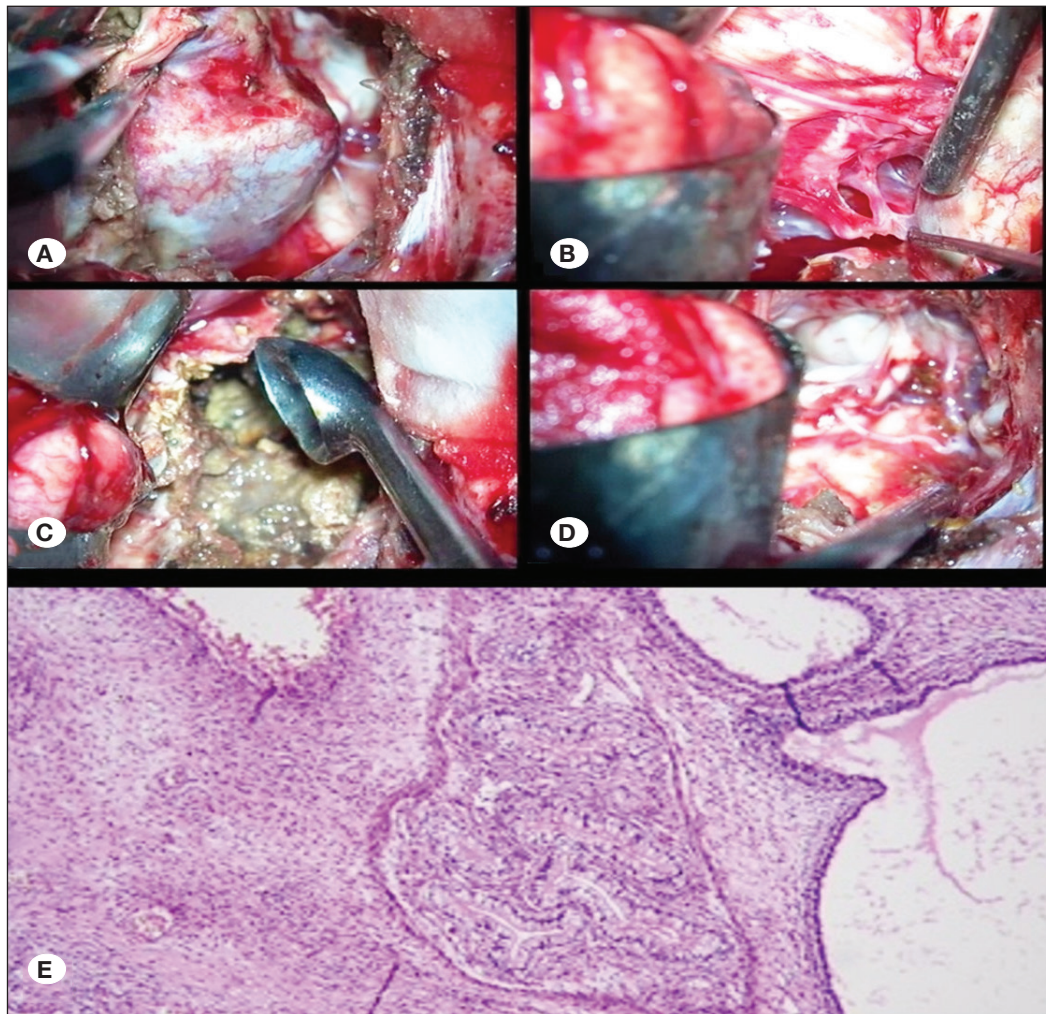


Figure 13: Patient #1. Posterior transcalsal teratoma located at the superior colliculus. **A)** Removal of the collicular component. **B)** Separation of vascular adherence. **C)** Tumor decompression. **D)** Total resection of the superior colliculus and pineal and cavum vergae components. **E)** Teratoma composed of multiple germ layers, including gastrointestinal-type glands lined with columnar epithelium. (H&E staining, $\times 200$).

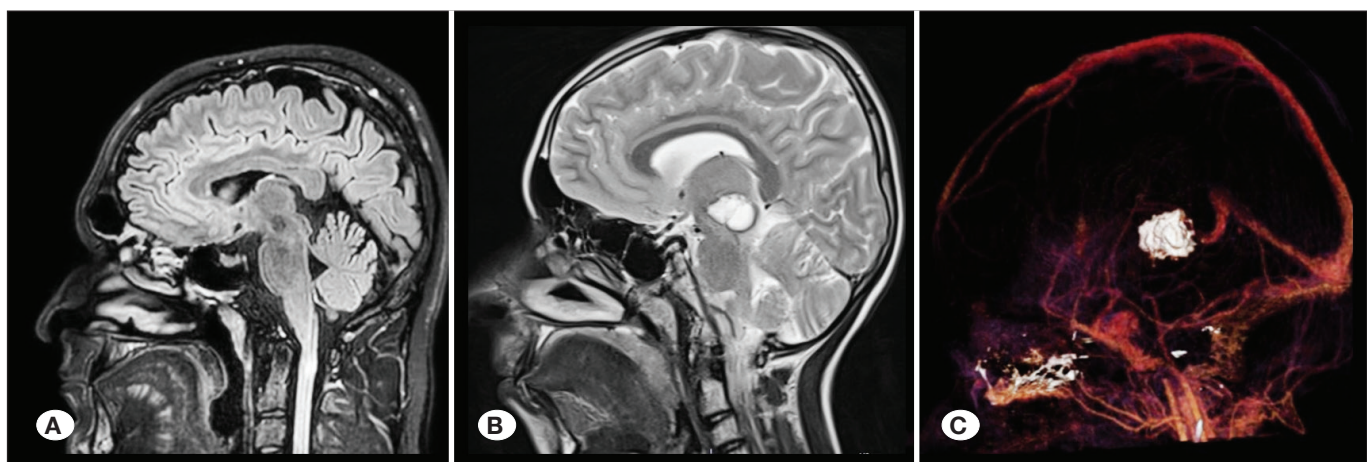


Figure 14: A tumor in the mesencephalon remaining indolent over several years [image(s) courtesy of the authors' archive].

gangliogliomas, gangliocytomas, or oligodendrogliomas or even PNETs (12). As observed in our cases, other conditions such as Parinaud's syndrome, head bobbing, Weber's syndrome, Benedict's syndrome, and strabismus can also be observed in patients with tectal tumors (1,23).

The midbrain has a perfect vascular structure (26). If tracts and nuclei are not damaged, then neurological deficits are not likely to occur. Sometimes, despite the development of hydrocephalus, computed tomography does not reveal a lesion (11) and can be misdiagnosed as idiopathic aquaeductus stenosis (25).

MRI enables the localization of tumors and identification of their histological characteristics, rendering biopsy nonessential to treatment (33). Sampling is inadequate in 35% of cases, and in 30%, it is inaccurate and lacks correlation with nondiagnostic results, resulting in 3% mortality and 4% morbidity. Stimulation of the trigeminal tractus results in an intense pain sensation (4). In instances where MRI displays atypical presentation and suggests the possibility of a noncancerous tumor, a diagnosis is typically made via an image-guided stereotactic biopsy in 96% of cases (14). DIPG is resistant to chemotherapy as macromolecules are unable to pass through an intact blood-brain barrier. Microantibodies (15) and cytokine overexpression occur in 70% of cases (23). Inhibiting agents are used, but

their effects remain controversial. Radiotherapy serves as the primary treatment modality (31).

Most medullary and cervicomedullary tumors are of focal and posterior exophytic types (28). They are demarcated and convenient for GTR; however, GTR is not recommended as most of these tumors are of low grade and pilocytic astrocytomas (20) (Figure 15).

Even after partial resection, patients can live for a long time independently (19). Anaplastic astrocytoma, GBM, ganglioglioma, ependymoma, hemangioma, oligoastrocytoma, and endothelioma are rare (18) (Figure 16).

In general, cervicomedullary tumors are unable to pass through the decussation pyramidalis and tractus; therefore, they push the medulla and fourth ventricle upward (28). At this site, the tumor becomes distorted and forms an exophytic portion by protruding posteriorly. The long tracts are also pushed and become flattened (28). This area can be used for the careful delivery of the tumor to the tracti (28).

Occasionally, the tumor extends to the decussation, fills the cisterna magna, and displaces the obex (28). It can also invade the CPA and attach to the 9th, 10th, and 11th cranial nerves (low group). Aspiration pneumonia may develop due to hydrocephalus and dysphagia (22). The children admit to

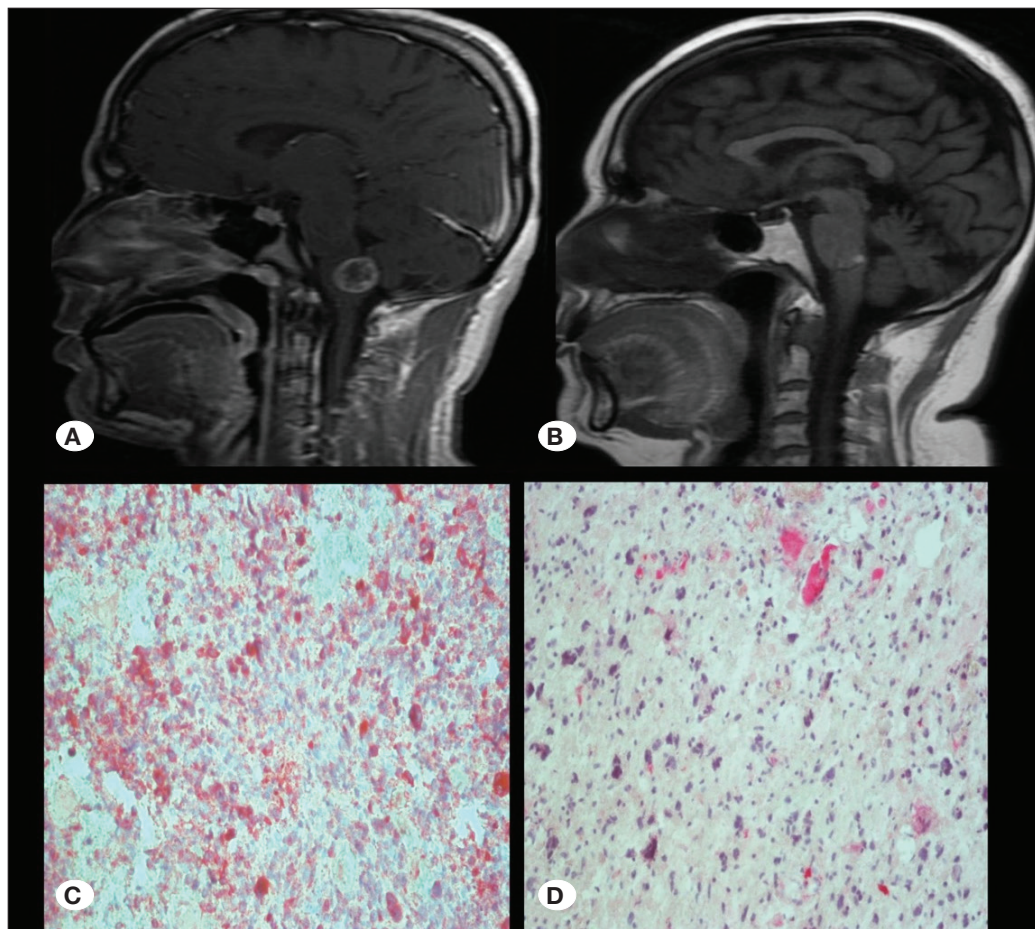


Figure 15: Patient #14. Medullary focal tumor. **A)** Preoperative sagittal T1W contrast enhanced MRI. **B)** Postoperative sagittal T1W MRI. **C)** Low-grade astrocytoma (H&E staining, $\times 100$), **D)** immunohistochemical staining, $\times 200$.

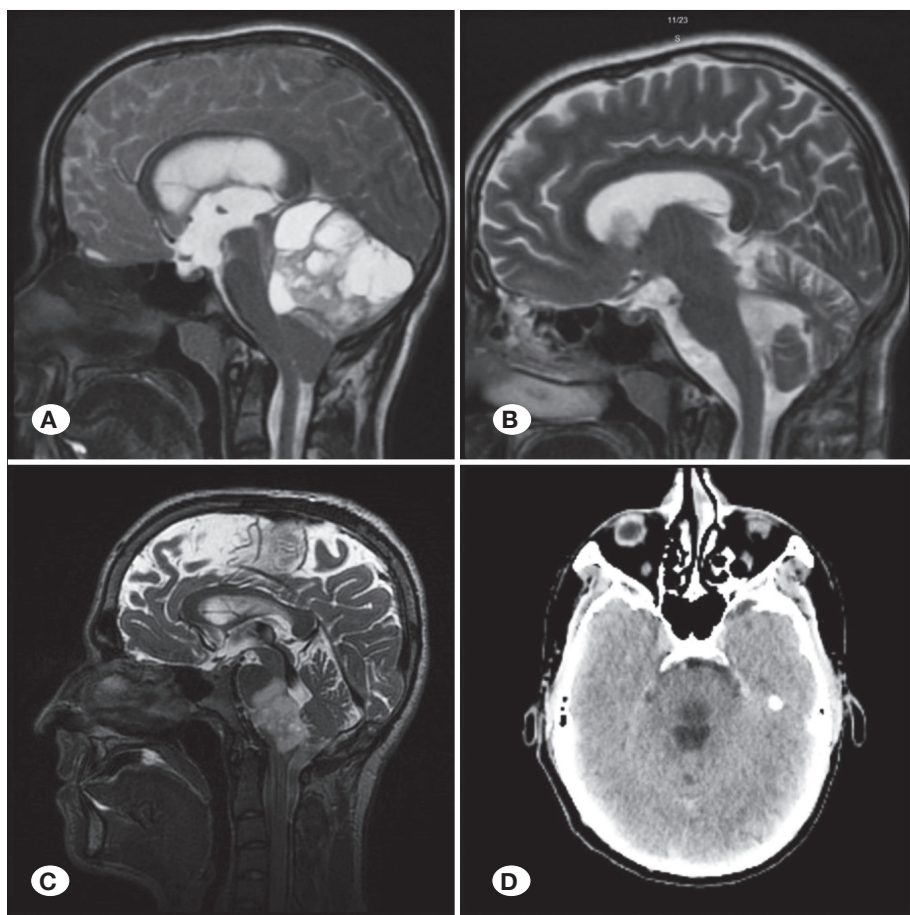


Figure 16: Patient #15. Dorsal exophytic medullary tumor. **A and C)** Preoperative T2W sagittal MRIs. Postoperative **B)** sagittal T2W MRI and **D)** axial CT images. No recurrence observed on postoperative imaging.

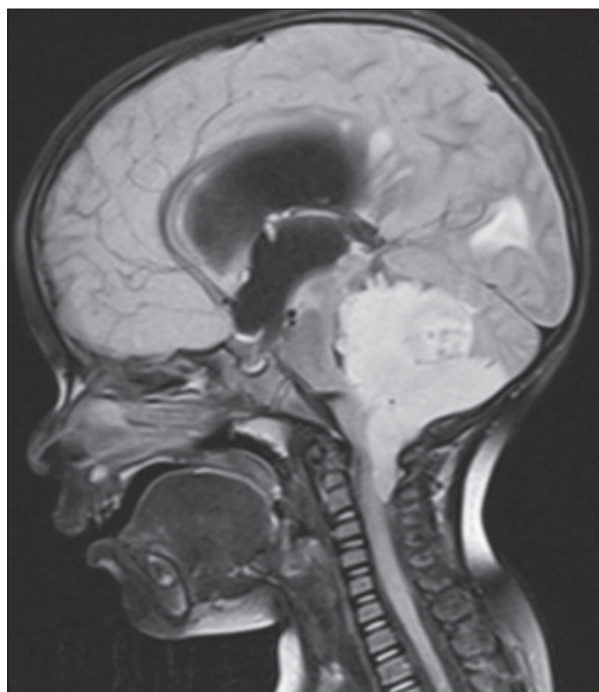


Figure 17: Cervicomedullary tumor exceeding the decussation pyramidalis and occupying the fourth ventricle, causing hydrocephalus in sagittal MR image [image(s) courtesy of the authors' archive].

gastroenterology and lung disease centers. The children have a long natural history, with 80% of them having headache with vomiting (27) (Figure 17).

In our patients with cervicomedullary tumors, the tumor passed decussation pyramidalis, filled cisterna magna, and displaced obex (28). Both patients had papillary stasis, and one had hydrocephalus. In one of our patients with cervicomedullary tumor, the tumor reached the PCA, involved the lower group, and caused dysphagia. This patient developed aspiration pneumonia and dysphagia and recovered in the first month. Almost all patients experienced headache. Notably, headache can be present with benign causes during childhood (27) (Figure 4).

Lateral exophytic medulla tumors have symptoms similar to those of PCA tumors and are resected through retromastoid craniectomy (22). Cysts and mural nodules are present in most of these tumors; furthermore, they expand to the subependymal area and displace the fourth ventricle (29). Tumors that fill the ventricles are resected in a similar manner to posterior fossa tumors (28). C1–2 laminectomy can be used based on the situation of the occiput and tonsil. For patients up to 4 years of age, the operation is performed in the prone position (28,29). For older children and adults, the operation is performed in the sitting position, taking precautions for air embolism. Because we are used to the

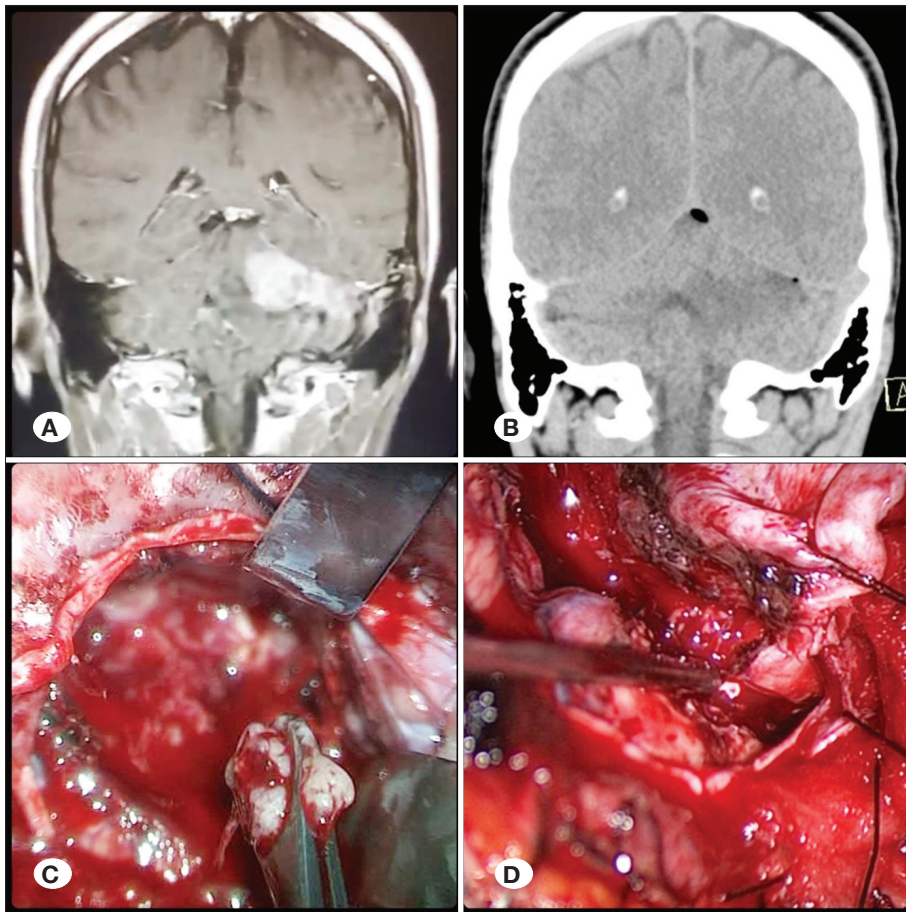


Figure 18: Patient #10. **A)** Preoperative T1W contrast enhanced coronal MRI. **B)** Postoperative coronal reconstructed CT scan. **C)** Piecemeal tumor removal. **D)** Gross total resection (GTR) confirmed.

sitting position, we preferred this for patients over 8 years old, with no complications other than pneumocephalus reported (22,28) (Figure 18).

The symptoms of cervicomedullary tumors are similar to those of spinal intramedullary tumors, and torticollis, irregular nocturnal breathing, and abscess can develop (28). They generally benefit from surgery. In one series 5 of 16 cases who underwent medulla and cervicomedullary junction surgery had favorable outcomes (28). A 38-year-old man was diagnosed with a focal medulla tumor, and GTR was performed in 2011. He was pathologically diagnosed with GBM. We recommended RT and chemotherapy and sent him to the oncology department (8). Subsequently, in 2017, he was admitted to our clinic due to the complaints of headache and vomiting (17); his MRI revealed tumor recurrence. Thus, we performed GTR again. Multiple metastases developed 1 year later; thus, we recommended chemotherapy (7) (Figure 19).

Of the seven patients who underwent surgery for cervicomedullary tumors, five had long tractus defect, two had hemiparesis, one had bilateral arm weakness, two had quadriplegia, and one had glossopharyngeal neuralgia and spasmodic torticollis. Based on these findings, we considered that the tumor involved the left lower cranial nerves (22).

Craniectomy was performed through a midline incision in the posterior fossa, and laminectomy was performed up to the C3 level. The bleeding tumor with intermedullary components was completely removed via resection, and temporary clips were applied during the procedure to areas with severe bleeding, where a possible vertebral aneurysm was suspected (28). After the GTR procedure, we removed the clips and exposed the fourth ventricle but found no evidence of a tumor. We then followed the VA to locate the glossopharyngeal neuralgia and identified and clipped a saccular aneurysm at the posterior inferior cerebral artery's exit (Figure 6).

We detected insignificant C7 hypoesthesia in two patients. Postoperatively, these patients developed left hemiparesis, and these symptoms resolved quickly after surgery.

We detected a cervicomedullary tumor in a 27-year-old man who had hypoesthesia on the left arm. He refused to undergo any operation. However, 3 months later, he was admitted to our clinic due to quadriplegia and dyspnea. Consequently, operation was performed urgently. We applied near-total resection with C2–3 laminectomy and midline cord incision. Postoperatively, deficits other than insignificant left hemiparesis resolved, but breathing distress at intervals of 5–6 h continued. On the 3rd day, irregular nocturnal breathing started (28). Tracheostomy was performed 1 week later, and he was pathologically diagnosed with GBM. Diaphragmatic

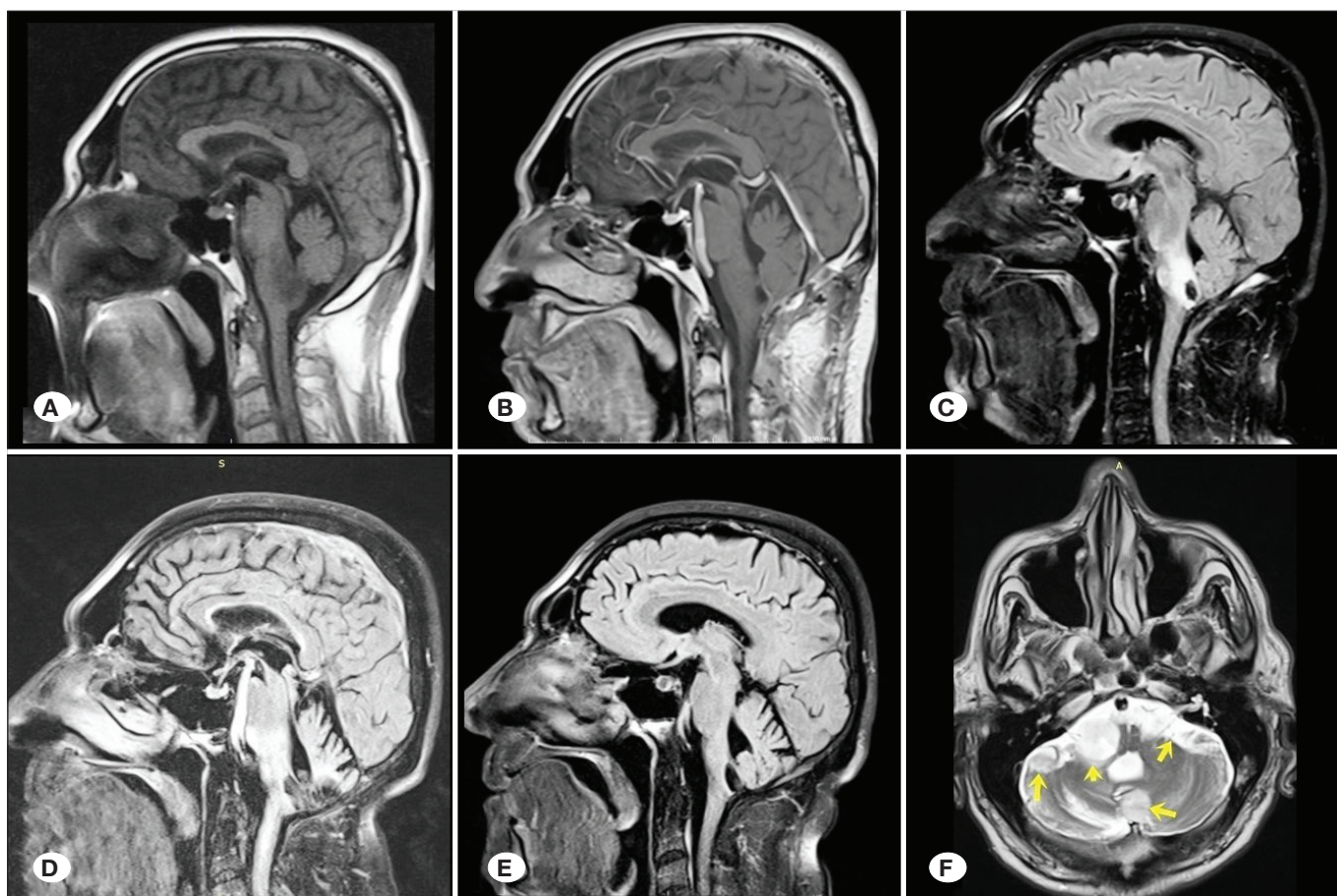


Figure 19: Patient #17. Medullary GBM. **A)** Preoperative sagittal T1W MRI at the time of diagnosis. **B)** T1W contrast enhanced sagittal MRI after first operation. **C)** FLAIR sagittal MRI after radiotherapy (2015). **D)** Sagittal T1W contrast enhanced MRI shows residual tumor (2018). **E)** FLAIR sagittal MRI after second operation. **F)** T2W axial MRI shows multiple metastatic lesions (2020).

respiration was insufficient, and the intercostal muscles were normal (Figure 3C-E).

Although Tsai and Rutka stated that recovery will be extremely slow, all symptoms resolved, except for breathing (28). Because of breathing distress, we could not apply RT and chemotherapy. At 2 months postoperatively, breathing support was provided at night. At the end of 2 months, proximal and distal tumor progression was detected. The patient died 2.5 months later due to respiratory arrest. Among the other two patients with medullary tumors, one with a cervicomedullary tumor developed recurrence within 3 years following RT and chemotherapy. Tsai and Rutka reported that 10%–20% of cervical tumors are of high grade (28). Two of our seven patients were diagnosed with GBM.

At times, it is impossible to differentiate tumor tissues from normal tissues surrounding the tumor (22). In this case, intraoperative MRI and USG can be used. However, due to the lack of opportunity, we performed frozen biopsy (29). In one case, we initially believed that the tumor had been completely removed; however, frozen biopsy of the surrounding tissue revealed astrocytoma grade II.

We avoided putting the patient at risk when the ultrasound imaging was unable to distinguish between the normal

and tumor tissues. Postoperative MRI revealed a near-total resection. In another case, cavernous malformation was observed at the medulla; moreover, bleeding tissues were detected at the base of the fourth ventricle, but no cavernomas were observed. We performed frozen biopsy and pathologically diagnosed astrocytoma grade II (29) (Figure 20).

We performed GTR. The primary treatment option for BST is surgical intervention. Surgical intervention enables histologic diagnosis, alleviates symptoms, removes the influence of the tumor mass, and decreases the numbers of malignant and stem cells. To obtain these effects, the tumor should be resected at least 10 ml (18,29).

BSTs must be subjected to GTR; however, caution must be exercised and this approach should not be insisted upon as most midbrain, medullary, and cervicomedullary tumors are focal, exophytic, and benign.

Partial, subtotal, and near-total resections enable free survival with longer prognosis (19,29). RT and chemotherapy are also effective. To demonstrate the benefits of chemotherapy, a reduction of at least 50% of the tumor volume should be observed. Operation should be performed with maximum exposure and minimum retraction. The aim should be maximum reduction (29).

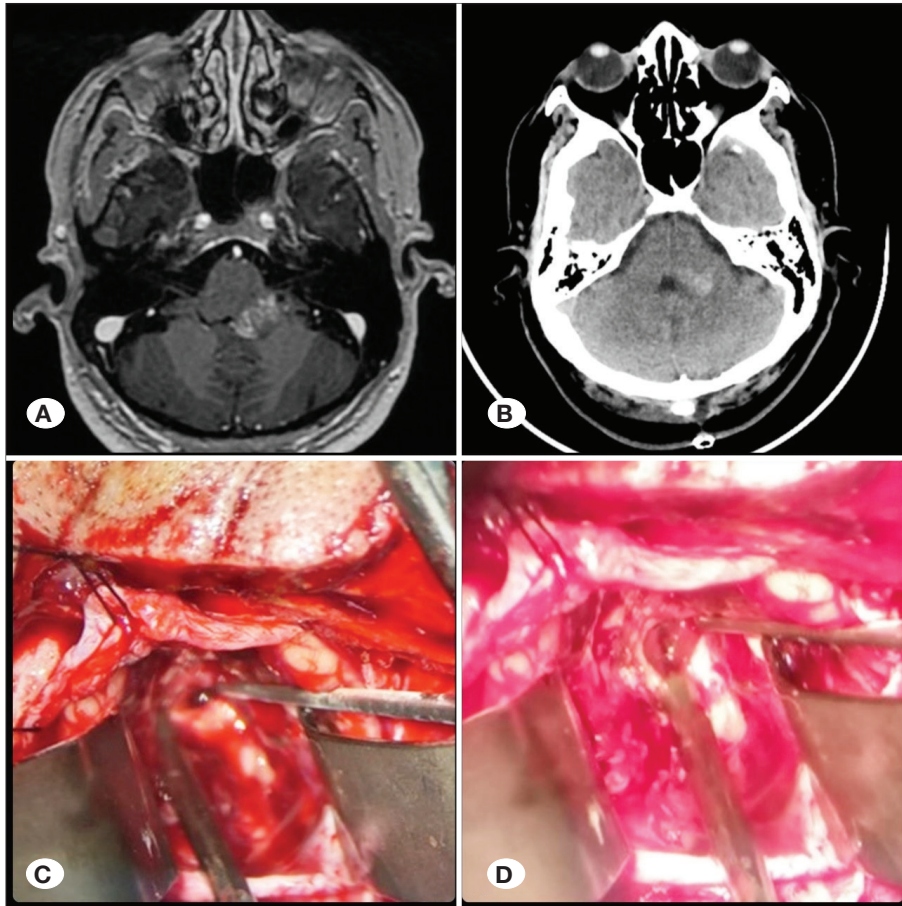


Figure 20: Patient #13. A cerebellar peduncular lesion initially suggestive of cavernoma; however, it was finally diagnosed as pilocytic astrocytoma. **A)** Preoperative T1W contrast enhanced axial MRI. **B)** Postoperative axial CT scan. Intraoperative views **C)** before and **D)** after resection. Final histopathology confirmed pilocytic astrocytoma.

Before opening the entrance to the tumor, the operation area should be examined using a microscope; the fourth ventricle and its base, subependymal cyst, discoloration, abnormal vascularization, bulging, protrusion, asymmetry, and displacement areas should be determined; and the shortest trajectory for entrance should be identified (20). Entrance through the medullary midline should be avoided due to the possibility of bilateral nuclear lesion development. Entrance from the cervicomedullary area should be preferred (28). Postoperatively, filling of the blood in the spinal canal can be mistaken for metastasis. Therefore, preoperative spinal MRI should be performed and compared with MRI performed on postoperative days 4–5 to confirm that the spinal canal is clear (28).

During the operation, to prevent the disruption of the tumor and avoid confusion with normal tissue under the microscope, thermal and biochemical coagulation using bipolar and laser techniques should not be applied to stop bleeding (28). The brainstem is highly sensitive to compression; therefore, mechanical hemostasis is provided mildly with a wet cotton compress. Normally, in the brainstem, perforating vessels exit with opposite angle to reduce the blood flow. Bleeding from vessels without laminin, fibronectin, and neuron can be stopped with mild compression; in cases where it does not work, Tisseel LYO (Baxter Turkey Renal Hizmetler A.S., İstanbul, Türkiye), fibrin sealant, can be used (28).

Using the posterior exophytic part of the medulla tumor as an entrance, the tumor can be removed up to the base of the fourth ventricle (22). A piecemeal technique can also be applied for the removal of tumors, which involves removing a tumor from the center to the periphery while staying within the tumor boundaries (22). If a cyst is present, it can be used as an entrance; a mural nodule should be totally resected (11).

In BSTs, a glial barrier is not present and the surrounding cuff is normal tissue; therefore, maximal care should be taken for this area (28).

Because flattened and distorted tracts are pushed even if they are not touched, their movement to the original area following tumor removal can lead to their damage (5).

We used nuclear and neuronal stimulators for BSTs (28). Although we did not receive a pathological stimulus from the monitor, we detected postoperative paresis of long tracts. Therefore, we aimed for spontaneous respiration from anesthesia in all patients with posterior fossa tumors. We halted the operation until the respiration and heart rhythm changes recovered. We terminated the operation in cases with frequent changes (28). The most important stimulus in operation was the deterioration in heart and respiratory rhythms. In cases where we were unsure about the differentiation of the tumor tissues from the surrounding tissues, we performed frozen section from a very small tissue.

As a result, if a tumor forms a place for itself by pushing the surrounding tissues, GTR can be applied if the entrance is found. However, infiltrative, invasive tumors that spread through the tractus are not amenable to safe resection; only their exophytic components can be removed (11,28)

CONCLUSION

Surgical treatment remains the cornerstone in the management of BSTs, offering histological diagnosis, mass effect elimination, symptom improvement, and cyst reduction. While GTR is the ideal treatment goal, it should not be insisted upon, particularly for midbrain, medullary, and cervicomedullary tumors that are often focal, exophytic, and benign in nature. In such cases, partial or subtotal resection can provide long-term survival with favorable outcomes.

Critical intraoperative considerations include vigilant monitoring of cardiac and respiratory parameters, maximal exposure with minimal retraction, and avoidance of aggressive maneuvers in infiltrative tumors. GTR is feasible when the tumor displaces surrounding tissue and allows a safe entry corridor; however, diffusely infiltrative tumors remain largely inoperable, aside from their exophytic components.

Our 13-year single-center experience suggests that individualized, anatomy-based surgical strategies, which are guided by neuromonitoring and advanced imaging, can lead to meaningful clinical improvement, even in complex cases.

ACKNOWLEDGEMENTS

The authors thank the neurosurgical and pathology teams involved in patient follow-up and data collection.

Declarations

Funding: This research did not receive any specific grant from funding agencies in the public, commercial, or not-for-profit sectors.

Availability of data and materials: The datasets generated and/or analyzed during the current study are available from the corresponding author by reasonable request.

Disclosure: The authors declare no competing interests.

AUTHORSHIP CONTRIBUTION

Study conception and design: EH

Data collection: EH, EY

Analysis and interpretation of results: EH, AED

Draft manuscript preparation: EH, EY, SH

Critical revision of the article: SH, EH

All authors (EH, EY, AED, SH) reviewed the results and approved the final version of the manuscript.

REFERENCES

- Albers AC, Gutmann DH: Gliomas in patients with neurofibromatosis type 1. *Expert Rev Neurother* 9:535-539, 2009. <https://doi.org/10.1586/ern.09.4>
- Amano T, Inamura T, Nakamizo A, Inoha S, Wu CM, Ikezaki K: Case management of hydrocephalus associated with the progression of childhood brain stem gliomas. *Childs Nerv Syst* 18:599-604, 2002. <https://doi.org/10.1007/s00381-002-0637-5>
- Asthağiri RA, Warren EK, Lonser RR: Brain tumors associated with neurofibromatosis. In: Kaye HA, Laws ER, (eds). *Brain Tumors*. Edinburgh: Elsevier; 2012:558-599. <https://doi.org/10.1016/B978-0-443-06967-3.00030-2>
- Başarı M, Özek MM: Beyin sapı tümörlerinde güncel tedavi seçenekleri. *Türk Nöroşir Derg* 26:43-51, 2016
- Bowers DC, Georgiades C, Aronson LJ, Carson BS, Weingart JD, Wharam MD, Melhem ER, Burger PC, Cohen KJ: Tectal gliomas: Natural history of an indolent lesion in pediatric patients. *Pediatr Neurosurg* 32:24-29, 2000. <https://doi.org/10.1159/000028893>
- Chico-Ponce de León F, Perezpena-Diazconti M, Castro-Sierra E, Guerrero-Jazo FJ, Gordillo-Domínguez LF, Gutiérrez-Guerra R, Salamanca T, Sosa-Sainz G, Santana-Montero BL, DeMontesinos-Sampedro A: Stereotactically-guided biopsies of brainstem tumors. *Childs Nerv Syst* 19:305-310, 2003. <https://doi.org/10.1007/s00381-003-0737-x>
- Di Maio S, Gul SM, Cochrane DD, Henderson G, Sargent MA, Steinbok P: Clinical, radiologic and pathologic features and outcome following surgery for cervicomedullary gliomas in children. *Childs Nerv Syst* 25:1401-1410, 2009. <https://doi.org/10.1007/s00381-009-0956-x>
- Donaldson SS, Laningham F, Fisher PG: Advances toward an understanding of brainstem gliomas. *J Clin Oncol* 24:1266-1272, 2006. <https://doi.org/10.1200/JCO.2005.04.6599>
- Dubey A, Patwardhan RV, Sampath S, Santosh V, Kolluri S, Nanda A: Intracranial fungal granuloma: Analysis of 40 patients and review of the literature. *Surg Neurol* 63:254-260, 2005. <https://doi.org/10.1016/j.surneu.2004.04.020>
- Farrell CJ, Plotkin SR: Genetic causes of brain tumors. *Neurol Clin* 25:925-946, 2007. <https://doi.org/10.1016/j.ncl.2007.07.008>
- Fisher PG, Breiter SN, Carson BS, Wharam MD, Williams JA, Weingart JD, Foer DR, Goldthwaite PT, Tihan T, Burger PC: A clinicopathologic reappraisal of brain stem tumor classification. Identification of pilocystic astrocytoma and fibrillary astrocytoma as distinct entities. *Cancer* 89:1569-1576, 2000. [https://doi.org/10.1002/1097-0142\(20001001\)89:7<1569::AID-CNCR22>3.0.CO;2-0](https://doi.org/10.1002/1097-0142(20001001)89:7<1569::AID-CNCR22>3.0.CO;2-0)
- Gupta M, Chan TM, Santiago-Dieppa DR, Yekula A, Sanchez CE, Elster JD, Crawford JR, Levy ML, Gonda DD: Robot-assisted stereotactic biopsy of pediatric brainstem and thalamic lesions. *J Neurosurg Pediatr* 27:317-324, 2021. <https://doi.org/10.3171/2020.7.PEDS20373>
- Greenberg ML, Fisher PG, Freeman C, Korones DN, Bernstein M, Friedman H, Blaney S, Hershon L, Zhou T, Chen Z, Kretschmar C: Etoposide, vincristine, and cyclosporin A with standard-dose radiation therapy in newly diagnosed diffuse intrinsic brainstem gliomas: A pediatric oncology group phase I study. *Pediatr Blood Cancer* 45:644-648, 2005. <https://doi.org/10.1002/xbc.20382>

14. Hamisch C, Kickingereder P, Fischer M, Simon T, Ruge MI: Update on the diagnostic value and safety of stereotactic biopsy for pediatric brainstem tumors: A systematic review and meta-analysis of 735 cases. *J Neurosurg Pediatr* 20:261-268, 2017. <https://doi.org/10.3171/2017.2.PEDS1665>
15. Joshi BH, Puri RA, Leland P, Varricchio F, Gupta G, Kocak M, Gilbertson RJ, Puri RK: Identification of interleukin-13 receptor $\alpha 2$ chain overexpression in situ in high-grade diffusely infiltrative pediatric brainstem glioma. *Neuro Oncol* 10:265-274, 2008. <https://doi.org/10.1215/15228517-2007-066>
16. Kawakami M, Kawakami K, Takahashi S, Abe M, Puri RK: Analysis of interleukin-13 receptor alpha2 expression in human pediatric brain tumors. *Cancer* 101:1036-1042, 2004. <https://doi.org/10.1002/cncr.20470>
17. Kaye HA, Laws ER: Historical perspective of brain tumor surgery. In: Kaye HA, Laws ER, (eds). *Brain Tumors*. New York: Elsevier, 2012:1-6. <https://doi.org/10.1016/B978-0-443-06967-3.00001-6>
18. Laigle-Donadey F, Doz F, Delattre JY: Brainstem gliomas in children and adults. *Curr Opin Oncol* 20:662-667, 2008. <https://doi.org/10.1097/CCO.0b013e32831186e0>
19. Lorincz KN, Gorodezki D, Schittenhelm J, Zipfel J, Tellermann J, Tatagiba M, Ebinger M, Schuhmann MU: Surgery in pediatric low-grade gliomas with brainstem involvement. *Childs Nerv Syst* 40:3037-3050, 2024. <https://doi.org/10.1007/s00381-024-06561-y>
20. Narayan P, Mapstone T: Dorsally exophytic brainstem gliomas. In: Berger MS, Prados MD, (eds). *Textbook of Neuro-Oncology*. Philadelphia: Saunders, 2005:634-637. <https://doi.org/10.1016/B978-0-7216-8148-1.50086-3>
21. Pollack IF: Intrinsic tumors of the brainstem. In: Batjer HH, Loftus CM, (eds). *Textbook of Neurological Surgery*. Philadelphia: Lippincott Williams & Wilkins, 2005:974-985.
22. Pollack IF, Hoffman HJ, Humphreys RP, Becker L: The long-term outcome after surgical treatment of dorsally exophytic brain-stem gliomas. *J Neurosurg* 78:859-863, 1993. <https://doi.org/10.3171/jns.1993.78.6.0859>
23. Robison NJ, Kieran MW: Diffuse intrinsic pontine glioma: A reassessment. *J Neurooncol* 119:7-15, 2014. <https://doi.org/10.1007/s11060-014-1448-8>
24. Salunke P, Sura S, Tewari MK, Gupta K, Khandelwal NK: An exophytic brain stem glioblastoma in an elderly presenting as a cerebellopontine angle syndrome. *Br J Neurosurg* 26:96-98, 2012. <https://doi.org/10.3109/02688697.2011.585670>
25. Samadani U, Judy KD: Stereotactic brainstem biopsy is indicated for the diagnosis of a vast array of brainstem pathology. *Stereotact Funct Neurosurg* 81:5-9, 2004. <https://doi.org/10.1159/000075097>
26. Serra C, Türe H, Firat Z, Staartjes VE, Yaltırık CK, Ekinci G, Sav A, Türe U: Microsurgical management of midbrain gliomas: Surgical results and long-term outcome in a large, single-surgeon, consecutive series. *J Neurosurg* 140:104-115, 2023. <https://doi.org/10.3171/2023.5.JNS222219>
27. Smith MA, Freidlin B, Ries LAG, Simon R: Trends in reported incidence of primary malignant brain tumors in children in the United States. *J Natl Cancer Inst* 90:1269-1277, 1998. <https://doi.org/10.1093/jnci/90.17.1269>
28. Tsai CE, Rutka JT: Cervicomedullary gliomas. In: Berger MS, Prados MD, (eds). *Textbook of Neuro-Oncology*. Philadelphia: Saunders, 2005:638-645. <https://doi.org/10.1016/B978-0-7216-8148-1.50087-5>
29. Upadhyaya SA, Koschmann C, Muraszko K, MD, Venneti S, Garton HJ, Hamstra DA, Maher CO, Betz BL, Brown NA, Wahl D, Weigelin HC, DuRoss KE, Leonard AS, Robertson PL: Brainstem low-grade gliomas in children—excellent outcomes with multimodality therapy. *J Child Neurol* 32:194-203, 2017. <https://doi.org/10.1177/0883073816675547>
30. Wang C, Zhang J, Liu A, Sun B, Zhao Y: Surgical treatment of primary midbrain gliomas. *Surg Neurol* 53:41-51, 2000. [https://doi.org/10.1016/S0090-3019\(99\)00165-2](https://doi.org/10.1016/S0090-3019(99)00165-2)
31. Warren KE, Killian K, Suuriniemi M, Wang Y, Quezado M, Meltzer PS: Genomic aberrations in pediatric diffuse intrinsic pontine gliomas. *Neuro Oncol* 14:326-332, 2012. <https://doi.org/10.1093/neuonc/nor190>
32. World Medical Association Declaration of Helsinki: ethical principles for medical research involving human subjects. *JAMA* 27;310(20):2191-2194, 2013. doi: 10.1001/jama.2013.281053
33. Yin L, Zhang L: Correlation between MRI findings and histological diagnosis of brainstem glioma. *Can J Neurol Sci* 40:348-354, 2013. <https://doi.org/10.1017/S0317167100014293>